RSC Advances

ROYAL SOCIETY OF CHEMISTRY

www.rsc.org/advances

Journal Name

RSCPublishing

ARTICLE

Near-infrared absorbing porphyrin dyes with perpendicularly extended π–conjugation for dye-sensitized solar cells

Cite this: DOI: 10.1039/xoxxoooooox

Received ooth January 2012,
Accepted ooth January 2012

DOI: 10.1039/xoxxoooooox

www.rsc.org/

Wenhui Li[†], Zonghao Liu[†], Xiaobao Xu[†], Yi-Bing Cheng[†‡], Zhixin Zhao[†]*, Hongshan He[§]*

Two new porphyrin dyes, coded as ZZX-N6 and ZZX-N6C12, with photon-to-electron response up to 800 nm in the solar spectrum were synthesized for dye-sensitized solar cells (DSCs). Four alkynyl groups were conjugated perpendicularly to the donor-π-acceptor axis of the porphyrins through triple bonds, resulting in 40~56 nm red-shift of absorption onset compared to porphyrin dye YD2-o-C8, leading to higher short-circuit current density. Post treatment of dye-coated TiO_2 films by chenodeoxycholic acid (CDCA) with a concurrent increase of iodide concentration in an electrolyte improved the cell performance. Both impedance spectroscopic and photovoltage decay measurements showed that charge resistance at the TiO_2/electrolyte interface increased after the CDCA treatment. Increasing iodide concentration in the electrolyte enhanced the reduction of I_3^- at the Pt counter electrode, leading to a higher short-circuit current density (J_{SC}) and a fill factor (FF). Under the optimized conditions, ZZX-N6 based device exhibited the energy conversion efficiency of 7.21%, which is comparable to YD2-o-C8 based device. The results demonstrate an alternative to broaden the light absorption capability of porphyrin dyes for high efficiency solar cells.

Introduction

Dye-sensitized solar cells (DSCs) as a low-cost, environmental friendly alternative to Si-based solar cells have drawn considerable attention in the past twenty years.[1-4] A typical DSC is consisted of a dye-sensitized working electrode, an electrolyte and a counter electrode in a sandwiched configuration. Ruthenium(II) bipyridyl complexes were the most efficient dyes; however, they suffer from high costs, low molar extinction coefficients, and weak absorption in the near-infrared (NIR) region limiting their photovoltaic performance.[1-4] A variety of alternative dyes have been developed. Among those, porphyrin dyes are attractive due to their versatile structural functionality for tuning photophysical properties. Recently, energy conversion efficiency exceeding 12% has been achieved in devices when porphyrin dyes (i.e. YD2-o-C8 and SM315) were used in conjunction with Co(II/III) electrolyte.[5,6]

The energy conversion efficiency of DSCs is largely dependent upon the light absorption capability of dyes. According to the energy distribution of the solar radiation, the NIR region accounts ~50% of the total energy. It is important to match the absorption spectra of dyes to the solar radiation in order to achieve better energy conversion efficiency. Though porphyrin dyes have intense absorption in the visible region, they usually show weak absorption in the NIR region.[7-15] Narrowing the energy gap between lowest unoccupied molecular orbital (LUMO) and highest occupied molecular orbital (HOMO) by extending the conjugated π-system along the donor-π-acceptor (D-π-A) axis is the most straightforward strategy. In 2007, Tanaka *et al.*[16] reported a naphthyl-fused zinc porphyrin achieving a red-shift of 131 nm compared to its unfused counterpart. The energy conversion efficiency is improved by 50%. Ball *et al.*[17] fused an anthracene into a porphyrin ring and extends the absorption to 900 nm. However, the resulting solar cell only produces less than 0.1% energy conversion efficiency due to unfavourable electron injection from its LUMO to the conduction band of TiO_2 nanoparticles. Diau and Lin *et al.*[18] found that inserting an anthracene between the donor and porphyrin ring extends the absorption edge over 750 nm giving efficiency between 8-10%. Here the balance between light absorption of dyes and electron injection from dyes to TiO_2 conduction is becoming crucial to achieving high efficiency.

It is rare to tune the energy level of frontier molecular orbitals through the extension of π-conjugation in the direction that is perpendicular to the D-π-A axis. In the state-of-the-art porphyrin dyes, these positions (*i.e.* two *meso* positions) are often used to attach bulky groups to suppress dye aggregation on the TiO_2 nanoparticles. Consequently, the potential of

extending π-conjugation in this direction vanishes. Previously we[19] found that bis(9,9-dihexyl-9H-fluorene-7-yl)amine as a donor is bulky enough to reduce the dye aggregation. To take this advantage, we describe a new strategy to extend the π conjugation through two *meso* positions that are perpendicular to the D-π-A axis. The structures of two new porphyrin dyes, coded as ZZX-N6 and ZZX-N6C12, are shown in Scheme 1. Different from YD2-o-C8, two dyes use a bis(9,9-dihexyl-9H-fluorene-7-yl)amine as an electron donor and another fluorene as a spacer. Two tris-isopropylsilane (TIPS) groups in ZZX-N6 were attached to the other end of the triple bonds to provide some hindrance to dye aggregation, whereas a fluorene with two *p*-dodecyloxylated phenyl groups in ZZX-N6C12 was used to replace the TIPS to further extend the π-conjugation and provide more hindrance. We expect this strategy will not only broaden the absorption spectra of the dyes, but also suppress the dye aggregation on the surface of TiO_2 nanoparticles.

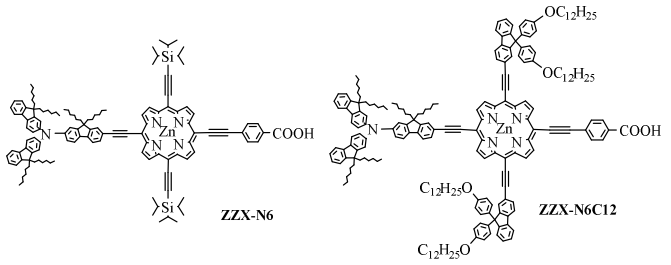

Scheme 1 Structure of ZZX-N6 and ZZX-N6C12.

Experiment section

General

All materials were commercially available and were used directly without further purification. Solvents used for reactions were dried by standard procedures. YD2-o-C8,[5] 5,15-dibromoporphyrinzinc (**2**),[20] 9,9-bis(4-hydroxyphenyl)-2-iodo-9H-fluorene,[21] and 2-(triisopropylsilyl)ethynyl-7-[bis(9,9-dihexyl-9H-fluorene-7-yl)amino]-9,9-dihexyl-9H-fluorene(**1**) were synthesized according to literatures.[19] Dye-loading amounts were obtained by de-adsorption of dyes from TiO_2 transparent films in a tetrabutylammoniumhydroxide solution and measurement of their absorption on a spectrophotometer.

SYNTHESIS OF 3

To a solution of **1** (1.31 g, 1.1 mmol) in 160 mL dry THF was added TBAF (1 M in THF, 6.6 mL). The mixture was stirred at room temperature in the dark for 45 minutes and then quenched by adding water. The mixture was extracted with CH_2Cl_2 and dried over anhydrous $MgSO_4$. The solvent was removed under reduced pressure. The residue was re-dissolved in a mixture of 120 mL dry THF and 20 mL dry TEA. After degassing with nitrogen for 30 minutes, $Pd(PPh_3)_2Cl_2$ (73.2 mg, 0.104 mmol), CuI (20 mg, 0.104 mmol) and **2** (892 mg, 1 mmol) were added to the mixture. The solution was then refluxed under nitrogen for 3.5h. The solvent was removed under reduced pressure. The residue was subjected to column chromatography (silica gel) using hexane/EtOAc = 30/1 as eluent. Recrystallization from CH_2Cl_2/MeOH gave **3** as a green solid. Yield:35.1%.^{1}H NMR(CD_2Cl_2, 400MHz) δ 9.63 (d, J=4.44Hz, 2H), 9.56 (d, J=4.48Hz, 2H), 9.37 (d, J=4.16Hz, 2H), 9.23 (d, J=3.84Hz, 2H), 8.15 (d, J=7.76Hz, 1H), 8.09 (s, 1H), 7.94 (d, J=7.76Hz, 1H), 7.69 (t, J=9.34Hz, 4H), 7.41 (m, 9H), 7.17 (t, J=8.00Hz, 3H), 2.00-2.29 (m, 12H), 1.57 (d, J=5.68Hz, 42H), 1.16-1.30 (m, 36H), 0.72-0.91 (m, 30H). MS (m/z, TOF) calcd for $C_{119}H_{148}BrN_5Si_2Zn$1850.0, found 1850.4.

SYNTHESIS OF ZZX-N6

Compound **3** (280 mg, 0.15 mmol) and 4-ethynylbenzoic acid (80 mg, 0.55 mmol) were dissolved in a mixture of dry THF (10 mL) and dry TEA (1.5 mL) and degassed with nitrogen for 15 minutes, then $Pd(PPh_3)_4$ (31 mg, 0.027 mmol), CuI (5 mg, 0.027 mmol) were added to the mixture. The solution was refluxed under nitrogen for 5h. The solvent was removed under reduced pressure. The residue was subjected to column chromatography (silica gel) using CH_2Cl_2/MeOH = 20/1 as eluent. Recrystallization from CH_2Cl_2/MeOH gave ZZX-N6 as a green solid. Yield: 80.1%.^{1}H NMR (CD_2Cl_2, 400MHz) δ 9.66-9.81 (overlapped, 8H), 8.28 (s, 2H), 8.17 (s, 2H), 8.10 (d, J=7.56Hz, 1H), 8.07 (s, 1H), 7.89 (d, J=7.68Hz, 1H), 7.65-7.74 (m, 4H), 7.32-7.43 (m, 9H), 7.14 (t, J=6.50Hz, 3H), 1.87-2.43 (m, 12H), 1.55 (d, J=5.76Hz, 42H), 1.15-1.26 (m, 36H), 0.70-0.94 (m, 30H). Elemental Analysis: calcd for $C_{128}H_{153}N_5O_2Si_2Zn$ C 80.27%, H 8.05%, N 3.66%; found C 80.31%, H 8.11%, N 3.64%. MS (m/z, TOF) calcd for $C_{128}H_{153}N_5O_2Si_2Zn$ 1915.2, found 1915.2.

SYNTHESIS OF 4

To a mixture of 9,9-bis(4-hydroxyphenyl)-2-iodo-9H-fluorene (476 mg, 1 mmol), K_2CO_3(249 mg, 1.8 mmol), KI (33.2 mg, 0.2 mmol) and acetone (10 mL) in a 25 mL flask was added n-bromododecane (0.53 mL, 2.2 mmol) under nitrogen. The mixtures were heated to reflux and stirred for 72h. After the reaction was cooled to room temperature, the mixture was poured into water and extracted with CH_2Cl_2. The organic extracts were washed with brine, dried over anhydrous $MgSO_4$, filtered and concentrated in *vacuo*. The resulting yellow oil was purified on silica gel chromatography using hexane/CH_2Cl_2 = 8/1 as eluent to give 600 mg of **4** as light yellow oil. Yield: 73.8%.^{1}H NMR ($CDCl_3$, 400MHz) δ 7.70 (m, 3H), 7.50 (d, J=8.00Hz, 1H), 7.32 (m, 3H), 7.08 (d, J=8.76Hz, 4H), 6.76 (d, J=8.80Hz, 4H), 3.91 (t, J=6.52Hz, 4H), 1.77 (m, 4H), 1.32 (m, 32H), 0.91 (m, 6H). MS (m/z, ESI) calcd for $C_{49}H_{65}IO_2$ 812.9, found 812.5 $[M]^+$.

SYNTHESIS OF ZZX-N6C12

To a solution of ZZX-N6 (19 mg, 0.01 mmol) in 2 mL dry THF was added TBAF (1M in THF, 0.2 mL). The mixture was stirred in dark at room temperature for 45 minutes and then quenched by water. The mixture was extracted with CH_2Cl_2 and dried over anhydrous Na_2SO_4.The solvent was removed under reduced pressure. The residue was dissolved in a mixture of 5mL dry THF and1.5 mL dry TEA and degassed with nitrogen for 0.5h; $Pd_2(dba)_3$ (5 mg, 0.0056 mmol), $AsPh_3$ (13.5 mg, 0.045 mmol) and **4** (81.3 mg, 0.1 mmol) were added to the mixture. The solution was stirred for 24h under nitrogen at room temperature. The solvent was removed under reduced

pressure. The residue was subjected to column chromatography (silica gel) using CH_2Cl_2/MeOH = 20/1 as eluent. Recrystallization from CH_2Cl_2/MeOH gave the ZZX-N6C12 as a green solid. Yield: 30.3%.^{1}H NMR (CD_2Cl_2, 400MHz) δ 6.48-9.31 (overlapped, 60H), 4.03 (s, 8H), 0.73-2.05 (overlapped, 178H). Elemental Analysis: calcd for $C_{208}H_{241}N_5O_6Zn$ C 84.04%, H 8.17%, N 2.36%; found C 84.12%, H 8.24%, 2.30%. MS (m/z, HRESIMS) calcd for $C_{208}H_{241}N_5O_6Zn$ 2972.6, found 1485.9 $[M/2Z]^+$.

Fabrication of solar cells

Working electrodes (an 8μm-thick transparent TiO_2 layer with a 3 μm-thick TiO_2 scattering layer) were dipped in a freshly prepared $TiCl_4$ aqueous solution at 70ºC for 30 minutes. The electrode was then flushed with de-ionized (DI) water, ethanol (EtOH), and dried with an air flow. Electrodes were then sintered at 500ºC for 30 minutes. After being cooled to 80ºC, the electrodes were immersed in the dye solutions (0.2 mM in THF for ZZX-N6 and ZZX-N6C12, and 0.2 mM in EtOH for YD2-o-C8, respectively) for 12 hours. The films were flushed with respective solvents thoroughly and dried in air for use. The counter electrodes were prepared by casting H_2PtCl_6 solution on clean FTO glass and sintered at 450ºC for 30 minutes. Two electrodes were sandwiched using a 45 μm thick hot-melt ring (Surlyn, DuPont). The internal space was filled with liquid electrolytes using a vacuum back filling system through pre-drilled holes on the counter electrode. The holes were sealed with a Surlyn sheet and a thin glass cover.

Device characterizations

Current-voltage cures were obtained by using an AM 1.5G solar simulator equipped with a 450 W xenon light (Oriel, model 9119) and an AM 1.5G filter (Oriel, model 91192). During the I-V measurement, a 0.09 cm^2 mask was used to get a uniform working area for all the cells. In the incident photon to electron conversion efficiency (IPCE) measurement, light from a 300 W xenon lamp (ILC Technology, U.S.A.) was focused through a Gemini-180 double monochromator (JobinYvon Ltd., U.K.) onto the cell under test. The monochromator was incremented through the visible spectrum to generate IPCE spectra. A white light bias (1% sunlight intensity) was applied onto the sample during the testing with an AC model (10 Hz).

Electrochemical impedance spectroscopy (EIS) and photovoltage decay measurements

Electrochemical properties were obtained on an Autolab Frequency Analyser set-up consisting of an Autolab PGSTAT 30 (Eco Chemie B.V., Utrecht, Netherlands) and a frequency response analyser module. Electrochemical impedance spectroscopy (EIS) was recorded in a frequency range of 10^{-1}-10^6 Hz. The determination of the interfacial recombination rate constant was carried out by performing transient photovoltage decay measurements and charge extraction experiments using a method from previous reports.[22-26]

Results and discussion

Scheme 2 shows the major synthetic steps for two porphyrin dyes. Compound 1 was prepared using a Sonogashira reaction as we described previously.[19] Compound 2 was prepared according to a method reported by Anderson *et al*.[20] Further reaction between compounds 1 and 2 gave intermediate 3, which was converted to ZZX-N6 and ZZX-N6C12 consecutively with yields 80.1 and 30.3%, respectively. Both compounds were fully characterized by NMR and high-resolution MS.

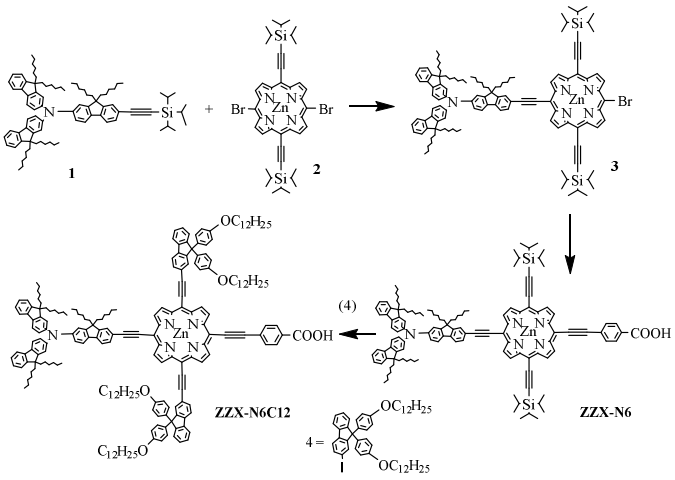

Scheme 2 Synthesis of ZZX-N6 and ZZX-N6C12

Absorption spectra ofZZX-N6 and ZZX-N6C12 in THF are shown in Fig. 1a with details in Table 1. Both dyes exhibited typical absorption features of porphyrin dyes with a strong Soret band and two moderate Q bands, corresponding to $S_0 \rightarrow S_2$ and $S_0 \rightarrow S_1$transitions, respectively.[27-29]The Soret band of ZZX-N6 and ZZX-N6C12 are centered at 478 and 496 nm, respectively. The Q bands of ZZX-N6 and ZZX-N6C12 are located at 686 and 702 nm, respectively. Both Soret and Q bands are significantly red-shifted compared to those of YD2-o-C8. The molar extinction coefficients of Q bands decreased in the order of ZZX-N6C12 > ZZX-N6 > YD2-o-C8.

Absorption spectra of ZZX-N6 and ZZX-N6C12 on TiO_2 films are shown in Fig. 1b. The spectra were obtained by dipping dye-sensitized working electrodes in a cuvette containing acetonitrile to mimic the real situation in devices. Upon adsorption onto TiO_2 films, ZZX-N6 and ZZX-N6C12 showed similar spectra changes compared to their absorption in solution. Both Soret and Q bands were broadened. The band broadening can be caused by either light scattering or dye aggregates. The working electrodes used in this measurement was comprised of ~ 20 nm TiO_2 particles only, and their scattering is negligible.[42] Therefore the band broadening was caused by dye aggregates. A blue-shift of Soret band was also observed. These results indicate that both ZZX-N6 and ZZX-N6C12 form H-type aggregation on TiO_2 films.[30-32, 43, 44]

Table 1 Electronic and electrochemical properties of ZZX-N6 and ZZX-N6C12.

Dyes	Absorption λ_{max}/nm (logε $M^{-1}cm^{-1}$)	Emission λ_{max}[a]/nm	E_{OX}[b] V(*vs.* NHE)	$E_{0\text{-}0}$[c] V(*vs.* NHE)	E_{OX}-$E_{0\text{-}0}$ (V)
ZZX-N6	686 (4.83) 628 (4.19) 478 (5.35)	696	1.19	1.85	-0.66
ZZX-N6C12	702 (4.94) 645 (4.24) 496 (5.51)	713	1.23	1.80	-0.57
YD2-o-C8[d]	645 (4.49) 581 (4.08) 448 (5.33)	663	0.82	2.11	-1.29

[a]ZZX-N6 was excited at 490nm and 506nm forZZX-N6C12; [b]Electrochemical measurements were performed at 25°C with each porphyrin (0.1 mM) in THF/0.1 M TBAP/N_2, GC working and Pt counter electrodes, Ag/AgCl reference electrode, scan rate=50mV/s; [c]Estimated from the intersection wavelengths of the normalized UV-vis absorption and the fluorescence spectra; [d]The data of YD2-o-C8 was obtained from reference 5.

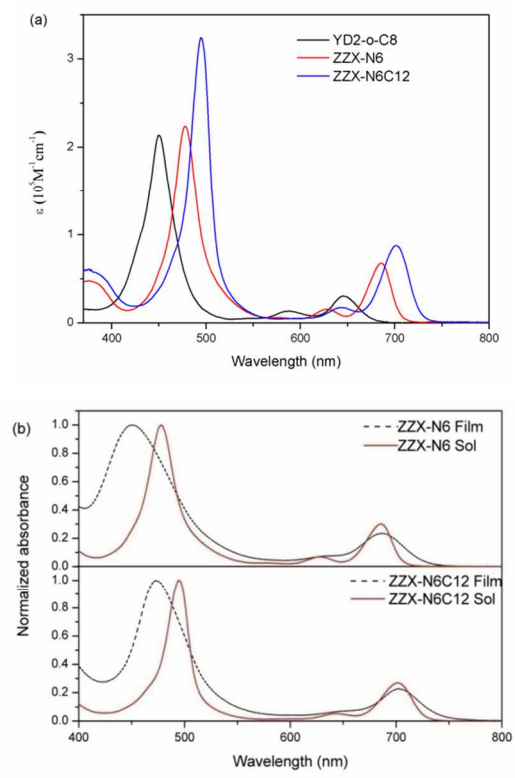

Fig. 1 Absorption spectra of ZZX-N6, ZZX-N6C12 andYD2-o-C8 in THF (a) and on TiO_2 films (b).

Cyclic voltammetry (CV) measurements and calculations were conducted to make sure if ZZX-N6 and ZZX-N6C12 can fulfill the basic energetic requirements of devices.[33] The detailed CV spectra in Fig. S1 (See ESI) and data in Table 1, oxidation potentials ($E(S/S^+)$) for ZZX-N6 and ZZX-N6C12 are 1.19 V and 1.23 V *vs.* NHE, respectively; both are much more positive than the redox potential of I/I_3^- (~0.5 V *vs.* NHE). From the intersection of the normalized absorption spectra and emission spectra, the zero–zero excitation energies ($E_{0\text{-}0}$) were obtained as 1.85 V and 1.80 V *vs.* NHE for ZZX-N6 and ZZX-N6C12, respectively. The reduction potentials ($E(S^*/S^+)$) were then determined from the relationship $E(S^*/S^+) = E(S/S^+)\text{-}E_{0\text{-}0}$, giving reduction potentials as -0.66 V and -0.57 V *vs.* NHE, respectively. The $E(S^*/S^+)$ are slightly more negative than the TiO_2 conduction band (-0.5 V *vs.* NHE). The results showed that the introduction of two extra alkynyl groups in the *meso* positions of the porphyrin ring effectively lowered the excited state extending the absorption band edge.

The photovoltaic performance of dyes was evaluated in Grätzel type devices. The dye loading time was fixed at 12h. It was found the ZZX-N6 sensitized cell exhibited 5.06% energy conversion efficiency with an open-circuit voltage (V_{OC}) of 536 mV and a short-circuit current density (J_{SC}) of 13.99 mA/cm^2. The efficiency was lower than we expected. We attributed this deficiency to the dye aggregation as evidenced by their absorption spectra on TiO_2 films. A cocktail dye-loading method (CT) was then used to overcome this problem. The CDCA was added to the dye solution during the dye loading process. The photovoltaic data of cells from this method were summarized in Table 2. It was found the addition of CDCA to the dye solution lowered the performance of ZZX-N6. The energy conversion efficiency decreased from 5.06 to 4.62, 4.22 and 3.14% when molar ratio of CDCA to ZZX-N6 increased from 0, 2, 6 and 10 as shown in Table 2. This decrease of efficiency stems from significant drop of J_{SC}. Dye loading density measurements showed that the density of ZZX-N6 on TiO_2 film decreased from 5.34×10^{-8} mol/cm^2 to 4.54×10^{-8} mol/cm^2 when the ratio of CDCA/dye increased from 0:1 to 2:1.

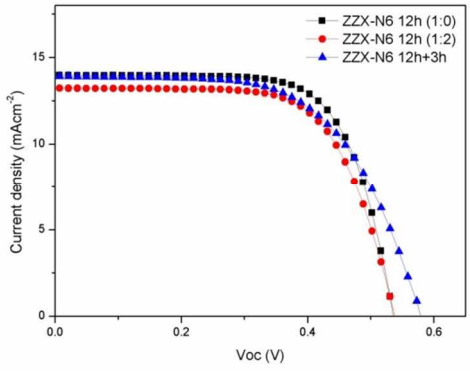

Fig. 2 Current-voltage curves of ZZX-N6 sensitized solar cells using CT method (coded as black and red lines) and a SQ method (coded as blue line).

Table 2 Cell performances of ZZX-N6 and ZZX-N6C12 sensitized solar cells from a cocktail and a sequential dye-loading method[a]

Electrolytes[b]	Dyes	Immersing time (h)[c]	V_{OC} (mV)	J_{SC} (mA/cm^2)	FF (%)	η (%)
		Cocktail Dye-loading Method				
A (0.03M I_2, no TBP)	ZZX-N6	12h (1:0)	536	13.99	69.62	5.06
		12h (1:2)	538	13.23	66.82	4.62
		12h (1:6)	540	10.86	71.56	4.22
		12h (1:10)	532	8.00	73.71	3.14
		Sequential Dye-loading Method				
A (0.03M I_2, no TBP)	ZZX-N6	12h+3h	579	13.91	60.40	4.72
		12h+9h	570	12.90	60.42	4.44
B (0.2M I_2, no TBP)	ZZX-N6	12h+3h	565	17.44	69.60	7.21
	ZZX-N6C12	12h+3h	516	14.88	69.63	5.63
	YD2-o-C8	12h+3h	602	7.97	68.49	3.29
C (0.03M I_2, 0.5M TBP)	ZZX-N6	12h+3h	701	8.39	65.17	4.03
	ZZX-N6C12	12h+3h	564	3.85	73.31	1.68
	YD2-o-C8	12h+3h	773	13.43	68.80	7.14

[a]Electrolyte A: 1.0M 1,3-dimethylimidazolium iodide, 0.03 M iodine, 0.05 M LiI, 0.1 M guanidiniumthiocyanate, in an 85:15 acetonitrile/valeronitrile;electrolyte B: 1.0 M 1,3-dimethylimidazolium iodide, 0.2M iodine, 0.05M LiI, 0.1 M guanidiniumthiocyanate, in an 85:15 acetonitrile/valeronitrile; electrolyte C: 1.0 M 1,3-dimethylimidazolium iodide, 0.03M iodine, 0.05M LiI, 0.1 M guanidiniumthiocyanate, 0.5M 4-*tert*-pyridine (TBP)in an 85:15 acetonitrile/valeronitrile; [b]Only the differences between three electrolytes were included; [c]The molar ratio of ZZX-N6 to CDCA is included in the parenthesis.

Alternatively, a sequential (SQ) dye-loading method was used to prepare photoelectrode. In the SQ method, the TiO_2 film was first immersed in a dye solution for 12h, followed by immersing in a 2.0M CDCA acetonitrile solution for three or nine hours. As shown in Fig. 2 and Table 2, three-hour post treatment by CDCA led to ~45 mV increase of V_{OC} with nearly no loss in short-circuit current density (J_{SC}) with the efficiency of 4.72%. When the post treatment time increased to nine hours, the efficiency dropped to 4.44%. The absorption spectra of dye-coated TiO_2 film recorded before and after CDCA treatment was shown in Fig. 3. It was found that the absorption intensity decreased after post CDCA treatment, which is in consistent with the drop in J_{SC} (see Table 2). The inset in Fig. 3 is the normalized absorption of Q bands before and after CDCA treatment. The absorptions were similar, but a slightly narrowed band width was observed after CDCA treatment indicating the dye aggregation was slightly reduced.

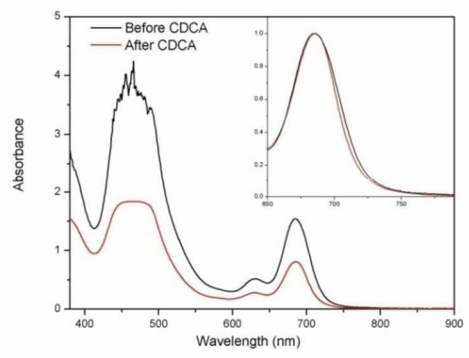

Fig. 3 Absorption spectra of ZZX-N6 coated films before and after a sequential CDCA treatment.

The post CDCA treatment may result several effects on alignment of dye molecules on the surface of the TiO_2 film. After being adsorbed onto TiO_2 nanoparticles, dye molecules likely align on the TiO_2 surface with a tilt angle as reported by Imahori *et al*.[34] As depicted in Fig. 4a, neighbouring molecules could overlap each other, resulting in aggregation or overlapping of molecules. Thus generates large voids between molecules. This will create opportunities for recombination of electrons on TiO_2 with I_3^- in electrolyte. The post CDCA treatment could exert three effects on cell performance: (i) inserting CDCA molecules between dye molecules, forming an insulating layer which effectively retarded the charge recombination between the injected electrons and I_3^- as demonstrated by EIS and photovoltaic decay measurements (see Fig. 5); (ii) removing of loosely bound dye molecules from TiO_2 surface. This will certainly reduce the fluorescence quenching; (iii) we noted that FF was lowered when post CDCA treatment was adopted as shown in Table 2, indicating that the resistance for mass transfer of redox couples was increased, and this should be an by-effect of increasing the compactness on the TiO_2 nanoparticle surface.

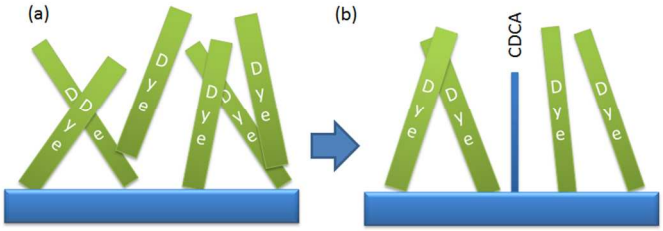

Fig. 4 Proposed dye interaction before (a) and after (b)CDCA treatment.

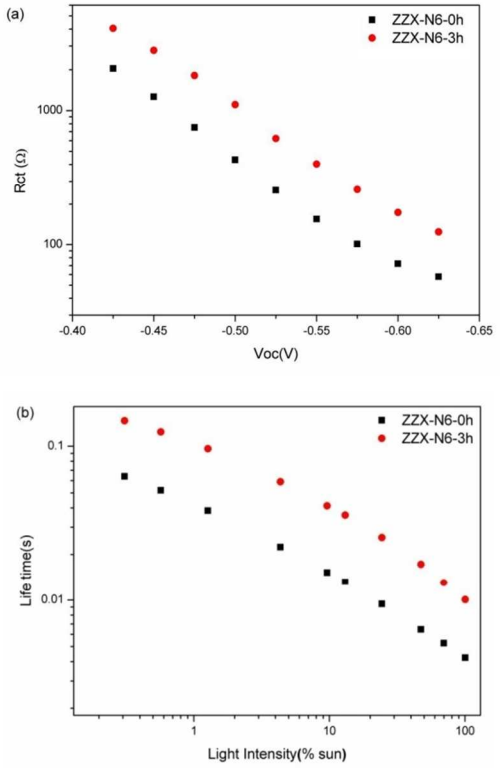

Fig. 5 (a) Comparison of Rct at certain Voc from EIS test in the dark; (b) Comparison of electron life times at certain light intensity from photovoltaic decay measurement.

The cell performance was increased significantly when the iodide concentration of electrolyte increased from 0.03 M to 0.2 M. The J_{SC} increased from 13.91 mA/cm^2 to 17.44 mA/cm^2 for ZZX-N6 sensitized cells. The *J-V* curves are shown in Fig. 6. Even though a 14 mV drop in V_{OC} was observed, the overall cell efficiency increased from 4.72% to 7.21%. The V_{OC} loss is ascribed to the side effect of increasing I_3^- concentration as more I_3^- means faster charge recombination at the TiO_2/electrolyte interface. It should be mentioned that the *FF* is generally higher in electrolyte B than in electrolyte A, which was also observed in multilayer systems as reported by Wang *et al*.[35] Increasing the iodide concentration could enhance the reduction reaction of I_3^- at the counter electrode, leading to higher J_{SC} and *FF* as observed in current work.

It was found that the ZZX-N6 exhibited higher efficiency than ZZX-N6C12 and YD2-o-C8 when the electrolyte B with higher I_2 concentration is used. Cells sensitized by ZZX-N6C12 and YD2-o-C8 were fabricated under the same condition using the SQ method and electrolyte B. The *J-V* curves were shown in Fig. 6. Table 2 listed the photovoltaic performance of ZZX-N6 and ZZX-N6C12 in the same cell fabrication conditions. Both ZZX-N6 and ZZX-N6C12 sensitized cells exhibited highest energy conversion efficiency by using electrolyte B. The ZZX-N6 sensitized cell exhibited the energy conversion efficiency of 7.21%, which is much higher than YD2-o-C8 (3.29%). The J_{SC} of DSCs can be calculated from the IPCE(λ) and the photon flux (Φ(λ)) incident on the cell:[36]

$$J_{sc} = e \cdot \int_{\lambda_{min}}^{\lambda_{max}} IPCE \cdot \Phi(\lambda)\, d\lambda \quad (1)$$

where e is the elementary charge and $\lambda_{min}\ldots\lambda_{max}$ defines a wavelength range where both of them are non-zero. One can easily get a conclusion from eq (1) that either extending the IPCE spectra or increasing the IPCE can lead to higher J_{SC}. The Fig.6b shows the IPCE action spectra of the devices. All devices showed typical characteristics of porphyrin based DSCs, exhibiting strong Soret and Q bands signals. The long-wavelength peaks of ZZX-N6 device and ZZX-N6C12 device were found to be red shifted into the NIR region cantered at ~710 nm and ~720 nm, respectively, while the IPCE of YD2-o-C8 device dropped rapidly in this region with a cut-off at ~720 nm. This result was in consistent with their absorption spectra. Because of the enhanced NIR absorbing ability, both ZZX-N6 B device and ZZX-N6C12 B device exhibited higher J_{SC} than YD2-o-C8 devices, which are consistent with their IPCE values. The desorption experimental showed that ZZX-N6 coated films exhibited higher dye loading compared to ZZX-N6C12 counterpart (5.34×10^{-8} mol/cm^2 and 4.53×10^{-8} mol/cm^2 for ZZX-N6 and ZZX-N6C12, respectively) due to its smaller size. Though the ZZX-N6 B device exhibited lower V_{OC} than YD2-o-C8 device using electrolyte C, it was compensated by its much higher J_{SC} (563 mV and 17.44 mA/cm^2 *vs.*773 mV and 13.43 mA/cm^2).

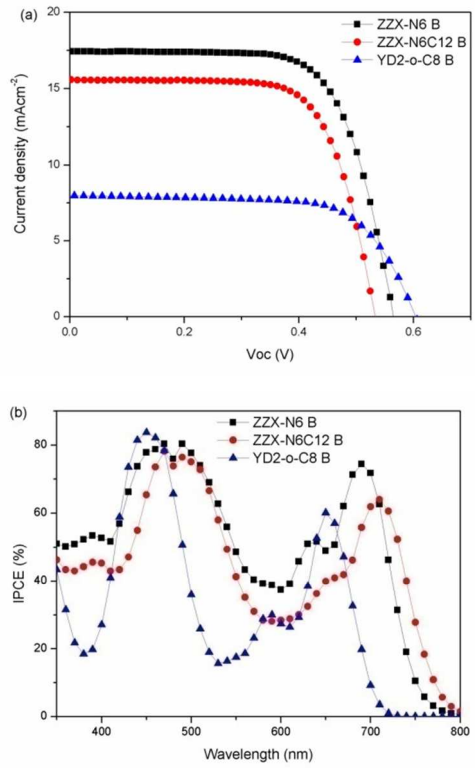

Fig.6 (a) Current-voltage curves; (b) IPCE spectra of the corresponding devices using a SQ method.

Transient photovoltage and charge extraction measurements were used to investigate the origin of the difference in V_{OC} between ZZX-N6 device and ZZX-N6C12 device. The decrease

in V_{OC} may originate from either (1) a downshift of the conduction band or (2) shorter electron lifetime resulting lower electron density in the conduction band.[37] As shown in Fig. 7a, the cells made with ZZX-N6 and ZZX-N6C12 feature nearly the same extracted charge (Q) at the same potential bias V_{OC}, ruling out a downshift of the conduction band as the origin of the decreased V_{OC} in ZZX-N6C12 device. Fig. 7b shows the lifetime of electrons as a function of charge density and ZZX-N6C12 device displayed shorter lifetime at a given charge density. It should be noted that the relative high lifetime observed here is due to the low electron density in the TiO_2 films.[45] The electron lifetime is determined by two time characteristics as described by following equation:[38]

$$\frac{\partial n}{\partial t} = G - \frac{n}{\tau_I} - \frac{n}{\tau_D} \qquad (2)$$

where τ_I and τ_D are the lifetimes determined by the recombination reactions between injected electrons and oxidized dye and I_3^-, respectively. The contribution from the former is negligible as the oxidized dyes are far more prone to react with I^- in the electrolyte.[39]

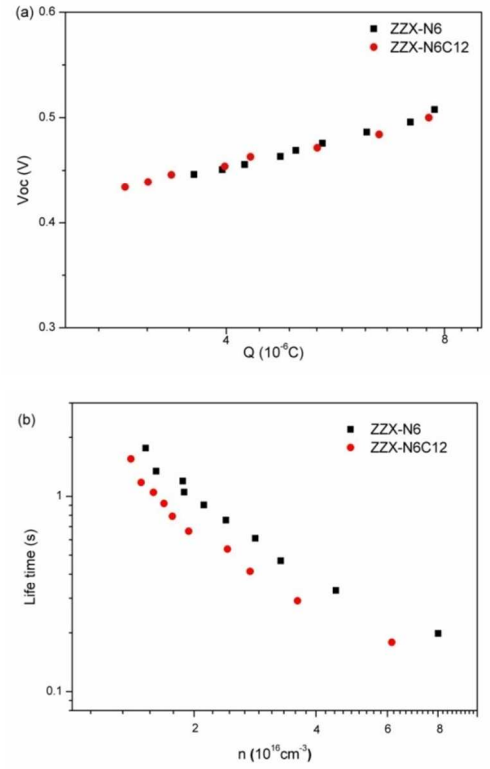

Fig. 7 (a) Comparison of the charges extracted from the porphyrin-grafted TiO_2films at a certain V_{OC}; (b)Electron lifetime against electron density.

We performed EIS measurement in the dark to obtain R_{ct}. In the dark condition, dyes at ground states cannot be excited and thus form oxidized dyes, so R_{ct} obtained here can be assumed to be equal with the recombination between electrons in the conduction band and I_3^-. As shown in Fig. 8, ZZX-N6C12 device exhibited smaller impedance for charge recombination suggesting faster recombination reaction in ZZX-N6C12 device. The enhanced recombination in ZZX-N6C12 implies that expanding the π-conjugation by replacing TIPS groups with fluorenyl groups is disadvantageous in suppressing charge recombination.

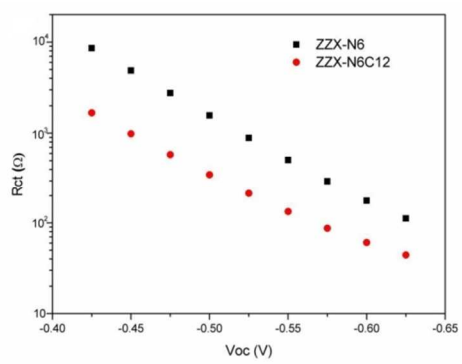

Fig. 8 Comparison of R_{ct} at certain V_{OC} from EIS tests in the dark.

It was found the energy conversion efficiency of ZZX-N6 and ZZX-N6C12 was very sensitive to 4-*tert*-butylpyrindine (TBP). The energy conversion efficiency of ZZX-N6 and ZZX-N6C12 was decreased when the TBP was added in the electrolyte. As shown in Table 2, ZZX-N6 sensitized cells showed 4.03% energy conversion efficiency when electrolyte C was used; whereas efficiency of YD2-o-C8 was 7.14%. Comparing to YD2-o-C8 sensitized cells, ZZX-N6 and ZZX-N6C12 sensitized cells showed lower Voc. The lower Voc mainly comes from the enhanced charge recombination at the TiO_2/electrolyte interface in ZZX-N6 and ZZX-N6C12 sensitized cells, as shown in Fig. 9. The lower energy conversion efficiency of ZZX-N6 and ZZX-N6C12 sensitized cells using electrolyte C should come from the smaller driving force for electron injection after adding 4-*tert*-butylpyridine to the electrolyte.[40,41]

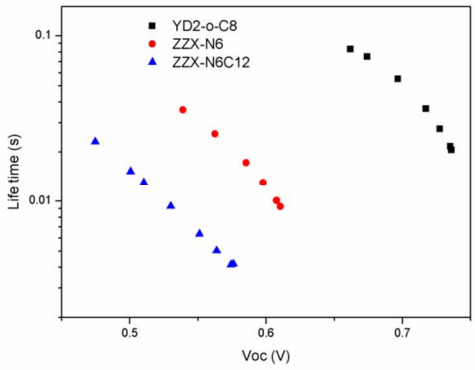

Fig. 9 Comparison of lifetimes of three porphyrins

Conclusion

Two new porphyrin dyes were synthesized to broaden the absorption of sunlight through direct conjugation of triple bonds to two *meso* positions of porphyrin ring. This strategy successfully red shifted the maximum absorption into the NIR

region. In efforts to improve cell performance, a sequential CDCA treatment was introduced to suppress the charge recombination at the TiO_2/electrolyte interface and restraining dye aggregation by increasing the compactness on the TiO_2 surface. Then electrolyte with higher I_2 concentration was used to accelerate the reduction of I_3^- at the electrolyte/Pt counter electrode interface. Conjunction of these two improvements increased the energy conversion efficiency of ZZX-N6 based devices from 5.06% to 7.21%, which is comparable to YD2-o-C8 sensitized cells. Considering the low Voc observed in these two new dyes based devices, further improvement in cell performance could be achieved by using Co(II/III) based electrolyte. The results also suggested that broadening the absorption to longer wavelength could result insufficient electron injection driving force during the cell operation. It is therefore of importance to balance the band edges to maximize the energy conversion efficiency.

Acknowledgement

This work was partially supported by the National Basic Research Program of China (973 program), Grant No. 2011CBA00703, the Fundamental Research Funds for the Central Universities, Grant No. HUST: 2014TS016 (Z.Z.) and Eastern Illinois University the President's Fund for Research and Creative Activity (H.H.). The authors thank one reviewer for valuable comments on the effect of sequential dye-loading method.

Notes and references

†Wuhan National Laboratory for Optoelectronics, Huazhong University of Science and Technology, Wuhan, 430074, China. E-mail:zhixin-zhao@hust.edu.cn.
§Department of Chemistry, Eastern Illinois University, Charleston, IL, USA. E-mail:hhe@eiu.edu
‡Department of Materials Engineering, Monash University, Melbourne, Victoria, 3800, Australia.

1 M. K. Nazeeruddin, F. D. Angelis, S. Fantacci, A. Selloni, G. Viscardi, P. Liska, S. Ito, B. Takeru and M. Grätzel, *J. Am. Chem. Soc.*, 2005, **127**, 16835–16847.
2 F. Gao, Y. Wang, D. Shi, J. Zhang, M. Wang, X. Jing, R. Humphry-Baker, P. Wang, S. M. Zakeeruddin and M. Grätzel, *J. Am. Chem. Soc.*, 2008, **130**, 10720–10728.
3 J. H. Yum, P. Walter, S. Huber, D. Rentsch, T. Geiger, F. Nüesch, F. D. Angelis, M. Grätzel and M. K.Nazeeruddin, *J. Am. Chem. Soc.*, 2007, **129**, 10320–10321.
4 H. Imahori, Y. Matsubara, H. Iijima, T. Umeyama, Y. Matano, S. Ito, M. Niemi, N. V. Tkachenko and H. Lemmetyinen, *J. Phys. Chem. C*, 2010, **114**, 10656–10665.
5 A. Yella, H.-W. Lee, H. N. Tsao, C. Yi, A. K. Chandiran, M. K. Nazeeruddin, E. W.-G. Diau, C.-Y. Yeh, S. M. Zakeeruddin and M. Grätzel, *Science*, 2011, **334**, 629−634.
6 S. Mathew, A. Yella, P. Gao, R. Humphry-Baker, B. F. E. Curchod, N. Ashari-Astani, I. Tavernelli, U. Rothlisberger, M. K. Nazeeruddin and M. Grätzel, *Nat. Chem.*, 2014, **6**, 242–247.
7 H.-P. Lu, C.-Y. Tsai, W.-N. Yen, C.-P. Hsieh, C.-W. Lee, C.-Y. Yeh, E. W.-G. Diau, *J. Phys. Chem. C*, 2009, 113, 20990–20997.
8 C.-P. Hsieh, H.-P. Lu, C.-L. Chiu, C.-W. Lee, S.-H. Chuang, C.-L. Mai, W.-N. Yen, S.-J. Hsu, E. W.-G. Diau and C.-Y. Yeh, *J. Mater. Chem.*, 2010, **20**, 1127–1134.
9 S.-L. Wu, H.-P. Lu, H.-T.Yu, S.-H. Chuang, C.-L.Chiu, C.-W. Lee, E. W.-G. Diau and C.-Y. Yeh, *Energy Environ. Sci.*, 2010, **3**, 949–955.
10 C.-W. Lee, H.-P. Lu, N. M. Reddy, H.-W. Lee, E. W.-G. Diau and C.-Y. Yeh, *Dyes and Pigments*, 2011, **91**, 317–323.
11 M. S. Kang, S. H. Kang, S. G. Kim, I. T. Choi, J. H. Ryu, M. J. Ju, D. Cho, J. Y. Lee and H. K. Kim, *Chem. Commun.*, 2012, **48**, 9349–9351.
12 N. M. Reddy, T.-Y. Pan, Y. C. Rajan, B.-C. Guo, C.-M. Lan, E. W.-G. Diau and C.-Y. Yeh, *Phys. Chem. Chem. Phys.*, 2013, **15**, 8409–8415.
13 K. Kurotobi, Y. Toude, K. Kawamoto, Y. Fujimori, S. Ito, P. Chabera, V. Sundström and H. Imahori, *Chem. Eur. J.*, 2013, **19**, 17075–17081.
14 S. H. Kang, M. S. Kang, I. T. Choi, J. Y. Hong, M. J. Ju and H. K. Kim, *ChemElectroChem*, 2014, **1**, 637–644.
15 H. Imahori, Y. Matsubara, H. Iijima, T. Umeyama, Y. Matano, S. Ito, M. Niemi, N. V. Tkachenko and H. Lemmetyinen. *J. Phys. Chem. C*, 2010, **114**, 10656–10665.
16 M. Tanaka, S. Hayashi, S. Eu, T. Umeyama, Y. Matano and H. Imahori, *Chem. Commun.*, 2007, 2069–2071.
17 J. M. Ball, N. K. S. Davis, J. D. Wilkinson, J. Kirkpatrick, J. Teuscher, R. Gunning, H. L. Anderson and H. J. Snaith , *RSC Adv.*, 2012, **2**, 6846–6853.
18 C.-L.Wang, J.-Y. Hu, C.-H. Wu, H.-H. Kuo, Y.-C. Chang, Z.-J. Lan, H.-P. Wu, E. W.-G. Diau and C.-Y. Lin, *Energy Environ. Sci.*, 2014, **7**, 1392-1396.
19W. Li, L. Si, Z. Liu, Z. Zhao, H. He, K. Zhu, B. Moore and Y.-B. Cheng, *J. Mater. Chem. A*, 2014, **2**, 13667–13674.
20T. E. O. Screen, K. B. Lawton, G. S. Wilson, N. Dolney, R. Ispasoiu, T. Goodson, S. J. Martin, D. D. C. Bradley and H. L. Anderson, *J. Mater. Chem.*, 2001, **11**, 312–320.
21 A. Sui, X. Shi, S. Wu, H. Tian, Y. Geng, F. Wang, *Macromolecules*, 2012, 45, 5436–5443.
22 C.-Y Chen, M. Wang, J.-Y. Li, N. Pootrakulchote, L. Alibabaei, C. Ngocle, J.-D. Decoppet, J.-H.Tsai, C. Grätzel, C.-G. Wu, S. Zakeeruddin and M. Grätzel, *ACS Nano*, 2009, **3**, 3103–3109.
23 M. Wang, J. Bai, F. L. Formal, S.-J. Moon, L. Cevey-Ha, R. Humphry-Baker, C. Grätzel, S. M. Zakeeruddin and M. Grätzel, *J. Phys. Chem. C*, 2012, **116**, 3266−3273.
24 B. C. O'Regan, S. Scully and A. C. Mayer, *J. Phys. Chem. B*, 2005, **109**, 4616-4623.
25 P. Tiwana, P. Docampo, M. B. Johnston, L. M. Herz and H. J. Snaith, *Energy Environ. Sci.*, 2012, **5**, 9566–9573.
26 B. C. O'Regan and F. Lenzmann, *J. Phys. Chem. B*, 2004, **108**, 4342−4350.
27 S. Verma, A. Ghosh, A. Das, H. N. Ghosh, *Chem. Eur. J.*, 2011, **17**, 3458–3464.
28 J. Rochford, D. Chu, A. Hagfeldt and E. Galoppini, *J. Am.Chem. Soc.*, 2007, **129**, 4655–4665.
29 J. Lu, X. Xu, K. Cao, J. Cui, Y. Zhang, Y. Shen, X. Shi, L. Liao, Y.-B. Cheng and M. Wang, *J. Mater. Chem. A*, 2013, **1**, 10008–10015.
30 C.-L.Wang, C.-M. Lan, S.-H. Hong, Y.-F. Wang, T.-Y. Pan, C.-W. Chang, H.-H. Kuo, M.-Y. Kuo, E. W.-G. Diau and C.-Y. Lin, *Energy Environ. Sci.*, 2012, **5**, 6933–6940.

31 N. C. Maiti, S. Mazumdar and N. Periasamy, *J. Phys. Chem. B*, 1998, **102**, 1528–1538.
32 U. Sigge, U. Bindig, C. Endisch, T. Komatsu, E. Tsuchida, J. Voigt, J.-H. Fuhrhop, *Ber. Bunsenges. Phys. Chem.*, 1996, **100**, 2070–2075.
33 A. Hagfeldt, G. Boschloo, L. C. Sun, L. Kloo and H. Pettersson, *Chem. Rev.*, 2010, **110**, 6595–6663.
34 H. Imahori, S. Hayashi, H. Hayashi, A. Oguro, S. Eu, T. Umeyama and Y. Matano, *J. Phys. Chem. C*, 2009, **113**, 18406–18413.
35 Z.-S. Wang, N. Koumura, Y. Cui, M. Takahashi, H. Sekiguchi, A. Mori, T. Kubo, A. Furube and K. Hara, *Chem. Mater.*, 2008, **20**, 3993–4003.
36 J. Halme, P. Vahermaa, K. Miettunen and P. Lund, *Adv. Mater.*, 2010, **22**, E210–E234.
37 A. J. Mozer, P. Wagner, D. L. Officer, G. G. Wallace, W. M. Campbell, M. Miyashita, K. Sunahara and S. Mori, *Chem. Commun.*, 2008, 4741–4743.
38 S. Nakade, T. Kanzaki, Y. Wada and S. Yanagida, *Langmuir*, 2005, **21**, 10803–10807.
39 D. Kuciauskas, M. S. Freund, H. B.Gray, J. R. Winkler and N. S. Lewis, *J. Phys. Chem. B*, 2001, **105**, 392–403.
40 K. Hara, Y. Dan-oh, C. Kasada, Y. Ohga, A. Shinpo, S. Suga, K. Sayama and H. Arakawa, *Langmuir*, 2004, **20**, 4205–4210.
41 G. Schlichthörl, S. Y. Huang, J.Sprague and A. J.Frank, *J. Phys. Chem. B*, 1997, **101**, 8141–8155.
42 J. Ferber and J. Luther, *Sol. Energy Mater. Sol. Cells*, 1998, **54**, 265–275.
43 M. Kasha, *Radiat. Res.*, 1963, **20**, 55–71.
44 C.-F. Lo, L. Luo, E. W.-G. Diau, I-J. Chang and C.-Y. Lin, Chem. Commun., 2006, 1430–1432.
45 A. Zaban, M. Greenshtein and J. Bisquert, *ChemPhysChem*, 2003, **4**, 859–864.

Two new near-infrared porphyrins exhibited energy conversion efficiency of 7.21% in dye-sensitized solar cells.